Bioconjugate Chemistry

Article

Cite This: Bioconjugate Chem. 2019, 30, 2011−2022

pubs.acs.org/bc

Kiss and Run: Promoting Effective and Targeted Cellular Uptake of a Drug Delivery Vehicle Composed of an Integrin-Targeting Diketopiperazine Peptidomimetic and a Cell-Penetrating Peptide

Lucia Feni,[†] Sara Parente,[‡] Clémence Robert,[‡] Silvia Gazzola,[‡] Daniela Arosio,[§] Umberto Piarulli,*[,‡] and Ines Neundorf*[,†]

[†]University of Cologne, Department of Chemistry, Biochemistry, Zülpicher Strasse 47a, D-50674 Cologne, Germany

[‡]Dipartimento di Scienza e Alta Tecnologia, Università degli Studi dell'Insubria, Via Valleggio 11, 22100, Como, Italy

[§]Istituto di Scienze e Tecnologie Molecolari (ISTM), National Research Council (CNR), Via G.Golgi 19, 20133, Milan, Italy

Supporting Information

ABSTRACT: Cell-penetrating peptides (CPPs) have emerged as powerful tools in terms of drug delivery. Those short, often cationic peptides are characterized by their usually low toxicity and their ability to transport diverse cargos inside almost any kinds of cells. Still, one major drawback is their nonselective uptake making their application in targeted cancer therapies questionable. In this work, we aimed to combine the power of a CPP (sC18) with an integrin-targeting unit (*c*[DKP-*f*3-RGD]). The latter is composed of the Arg-Gly-Asp peptide sequence cyclized via a diketopiperazine scaffold and is characterized by its high selectivity toward integrin $\alpha_v\beta_3$. The two parts were linked via copper-catalyzed alkyne−azide click reaction (CuAAC), while the CPP was additionally functionalized with either a fluorescent dye or the anticancer drug daunorubicin. Both functionalities allowed a careful biological evaluation of these novel peptide-conjugates regarding their cellular uptake mechanism, as well as cytotoxicity in $\alpha_v\beta_3$ integrin receptor expressing cells versus cells that do not express $\alpha_v\beta_3$. Our results show that the uptake follows a "kiss-and-run"-like model, in which the conjugates first target and recognize the receptor, but translocate mainly by CPP mediation. Thereby, we observed significantly more pronounced toxic effects in $\alpha_v\beta_3$ expressing U87 cells compared to HT-29 and MCF-7 cells, when the cells were exposed to the substances with only very short contact times (15 min). All in all, we present new concepts for the design of cancer selective peptide−drug conjugates.

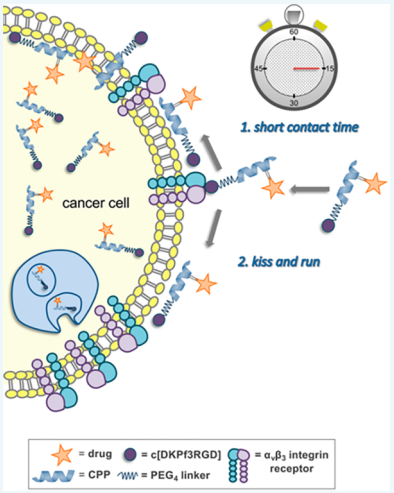

INTRODUCTION

The deeper understanding of oncogenic molecular mechanisms has provided new perspectives in the development of efficient antitumor therapies. In the past few years, cancer research has dramatically evolved, particularly with the advent of targeted molecular therapies[1−4] and advances in immunotherapy[5−7] that allowed the discovery and validation of innovative molecules, more effective and less harmful than conventional chemotherapy. This fervor is demonstrated by several new FDA-approved treatment strategies including immune check-point inhibitors,[8] adoptive T-cell therapy,[9] and the approval of helpful diagnostic tests to prognosticate the right targeted therapeutic to each patient.[10] As a consequence, the clinical practice guidelines changed a lot over the past two decades. Despite all this progress, cancer is still a leading cause of death worldwide.[11] Indeed, malignant cells often escape these treatments, or develop resistance, so an improvement of the therapeutic index remains a necessary goal.

One major obstacle of anticancer compounds is their inability to cross body barriers, especially cell membranes. Cell permeability of a drug has therefore been considered as a key step for therapeutic efficacy. This need in successful drug delivery has paved the way for the development of different drug delivery strategies, including lipid- or peptide/protein-based nanocarriers, inorganic vehicles, or other polymeric carriers.[12] In recent years, cell-penetrating peptides (CPPs) emerged as a potent tool for intracellular delivery of bioactive compounds also in the field of tumor diagnosis and therapy.[13] CPPs are usually short, cationic, and/or amphipathic peptides that are able to autonomously transverse plasma membranes either by direct permeation or via endocytotic processes, without the need for auxiliary proteins such as transporters. In this context, promising new CPP sequences have been identified and applied as vehicles for bioactive molecules like oligonucleotides, peptides, metal−organic complexes, and nanoparticles.[14] One major drawback of these peptides is their unselective uptake in nearly all cell types. For this reason, endowing CPPs with cell-selectivity, especially for future *in vivo* applications in cancer diagnosis or therapy, is a

Received: April 22, 2019
Revised: May 24, 2019
Published: June 3, 2019

DOI: 10.1021/acs.bioconjchem.9b00292
Bioconjugate Chem. 2019, 30, 2011−2022

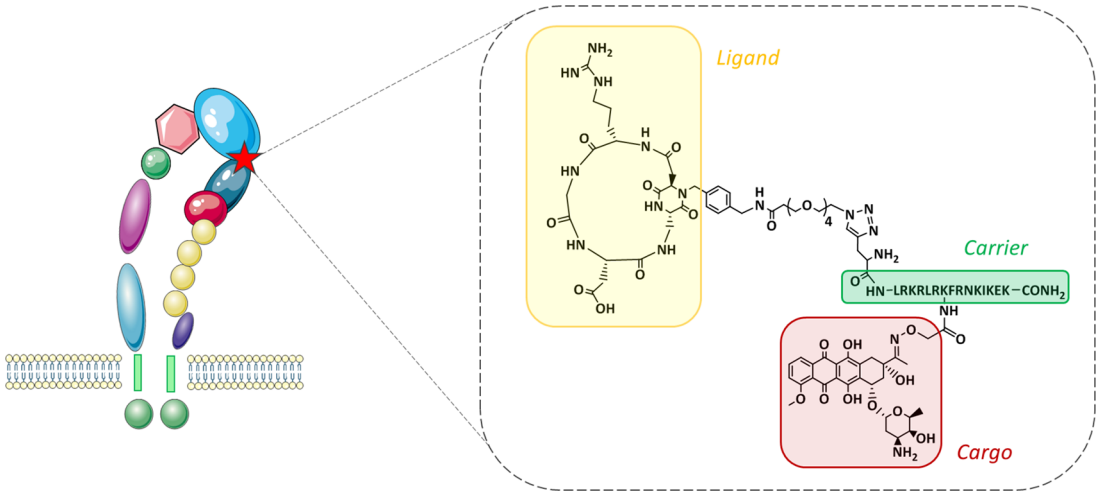

Figure 1. Graphical model describing the setup of the new drug delivery system studied within this work.

key factor in the development of these peptides. Recent progress has been made by developing pH-responsive,[15] or masked CPPs, by making advantage of their cationic nature,[16] or by fusion with peptides that act as targeting units.[17]

Other targeted anticancer therapies include antibody–drug conjugates (ADCs), which are specifically designed to act on cancer cells with a selective, potent mechanism, targeting tumor cells expressing surface antigens essential for their growth and survival.[18] Their antitumor efficacy and excellent tolerance profile have allowed targeted molecular therapies to quickly become therapeutic standards for many neoplastic conditions.[19] However, often tumors develop mechanisms of resistance, and the clinical benefit of these treatments remains limited over time.[20] In addition, ADCs have shown some important limitations such as high unfavorable pharmacokinetics (low tissue diffusion and low accumulation rate) and possible immunogenicity with respect to targets located outside the circulatory system and inside the cells, together with high manufacturing costs and the need of a challenging chemical synthesis.[21] Therefore, small-molecule drug conjugates have become of particular interest;[22] among those, peptide–drug conjugates were developed, that, in contrast to ADCs, are characterized by a deep tissue penetration, the possibility of targeting inside the cells, and relatively easy synthetic pathways.[23]

In the context of selectivity, integrins have received significant attention as potential targets in cancer treatment.[24] Integrins are heterodimeric cell-transmembrane glycoproteins consisting of α and β subunits. Depending on the combination of the different α and β subunits, their ligand binding specificity, signaling properties, and their affinity to endogenous proteins of the extracellular matrix is determined. Integrins play major roles in various cellular processes like cell adhesion, migration, and cell proliferation even if the different biological functions of the subtypes are only partially known. In particular, integrins $\alpha_v\beta_3$ are overexpressed on the surface of some tumor cells, influencing the malignant potential of a tumor as well as host cell response to cancer, being involved in tumor angiogenesis and metastasis.[25,26] These integrins recognize and bind the tripeptide sequence RGD in their natural ligands, and several low nanomolar peptidic ligands bearing this sequence have been developed so far.[27,28] Thanks to their excellent binding, RGD integrin ligands have also been often used as very efficient targeting units,[29−31] although in some cases the ability of these ligands to enhance efficient tumor penetration has been matter of debate.[27,32−36]

In this work, we elucidated the concept of combining the power of cell-penetrating peptides with the selectivity of an integrin receptor ligand, with the aim to develop a peptide–drug conjugate actively targeting tumor cells. In particular, the new drug delivery system (DDS) is composed of a CPP, namely, sC18,[37] and an integrin ligand (*c*[DKP-RGD])[38,39] characterized by its high selectivity toward integrin $\alpha_v\beta_3$. For proof-of-principle, the anticancer drug daunorubicin (dau) was used as cytotoxic payload and covalently linked to the CPP by oxime ligation. Daunorubicin is frequently applied as a toxin in cancer treatment and research, and was thus used within this study. Although it is characterized by high toxic potency, it lacks selectivity, and therefore, safe and targeted delivery of this toxin to the tumor cells would be preferable.[40−42] The generated products combine a highly selective homing device with the merits of an efficient drug delivery vehicle (Figure 1).

RESULTS AND DISCUSSION

Synthesis of the Peptide–Drug Conjugates. Scheme 1 summarizes all CPP variants that were used to build up the targeted DDS. The peptide sequence of sC18 was prepared by automated SPPS, introducing at position 8 a lysine residue, orthogonally protected as 1-(4,4-dimethyl-2,6-dioxocyclohex-1-ylidene)ethyl derivative (Dde), to provide an attachment point for 5(6)-carboxyfluorescein (CF), for cellular uptake studies, and daunorubicin (dau), to obtain a drug-loaded peptide conjugate. In addition, a *N*-terminal propargylglycine was introduced, for subsequent chemical ligation to the integrin ligand moiety via copper-catalyzed azide–alkyne click reaction (CuAAC). This approach has been already adopted in our group for the synthesis of triazole-containing cyclic peptides,[43,44] and the protocol used herein for CuAAC was recently established for the preparation of RGD peptidomimetic–paclitaxel conjugates.[45] Daunorubicin (dau) was conjugated to sC18 via oxime ligation, using aminooxyacetic acid (Aoa) as linker.[46] Oximes and hydrazones have been used for the preparation of prodrugs and conjugates of anthracyline drugs (such as daunorubicin and doxorubicin) because they are normally stable at physiological pH, while being rapidly cleaved at pH lower than 5.5, which is encountered inside tumor cells.[47] To facilitate the release of

DOI: 10.1021/acs.bioconjchem.9b00292
Bioconjugate Chem. 2019, 30, 2011−2022

Scheme 1. (A) Exemplifies the Synthesis of the CPP Precursors That Were Differently Functionalized for Later Biological Studies[a]. (B) Highlights the Synthesis of Two Further Precursors (IV and V) That Were Used to Generate Compounds 3b and 3c, Respectively[b]

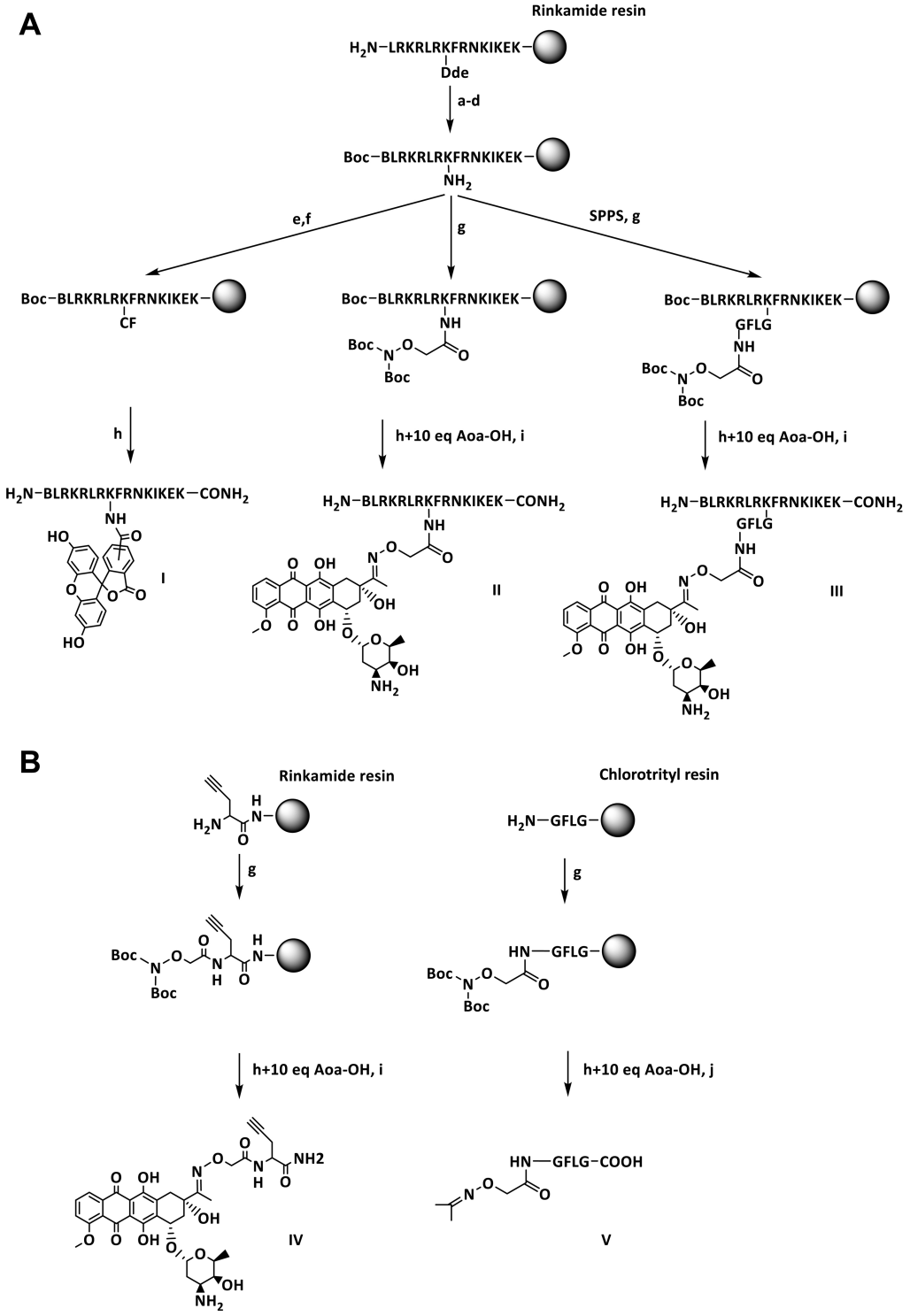

[a]**a**: 5 eqiv Fmoc-L-propargylglycine−OH (B), 5 equiv Oxyma, 5 equiv DIC in DMF, overnight; **b**: 30% piperidine in DMF (20 min × 2); **c**: 10 equiv Boc_2O, 1 equiv DIPEA in DCM for 2 h (2×); **d**: 2% hydrazine in DMF (10×); **e**: 2 equiv CF, 2 equiv HATU, 2 equiv DIPEA in DMF for 2 h, then 5 equiv CF, 5 equiv Oxyma, 5 equiv DIC in DMF overnight; **f**: 20% piperidine in DMF, 45 min; **g**: 5 equiv Bis-Boc aminooxy acetic acid, 5 equiv Oxyma, 5 equiv DIC in DMF, overnight; **h**: TFA/TIS/H_2O (95:2.5:2.5); **i**: 30% excess daunorubicin, 0.2 M NH_4OAc, pH 5, 10 mg/mL; **j**: acetone, rt, 30 min. [b]See also Scheme 2 (B: propargylglycine; Aoa−OH: aminooxyacetic acid).

daunorubicin from the DDS further, we introduced the Gly-Phe-Leu-Gly sequence between the drug and the peptide carrier. This sequence represents the recognition and cleavage site of Cathepsin B, a lysosomal cysteine protease, which is highly overexpressed in a wide variety of human cancers.[48] The Gly-Phe-Leu-Gly sequence was introduced between the drug and the

DOI: 10.1021/acs.bioconjchem.9b00292
Bioconjugate Chem. 2019, 30, 2011−2022

Scheme 2. Synthesis of the Full Conjugates 1, 1a, 1b, 1c, and 3b, 3c[a]

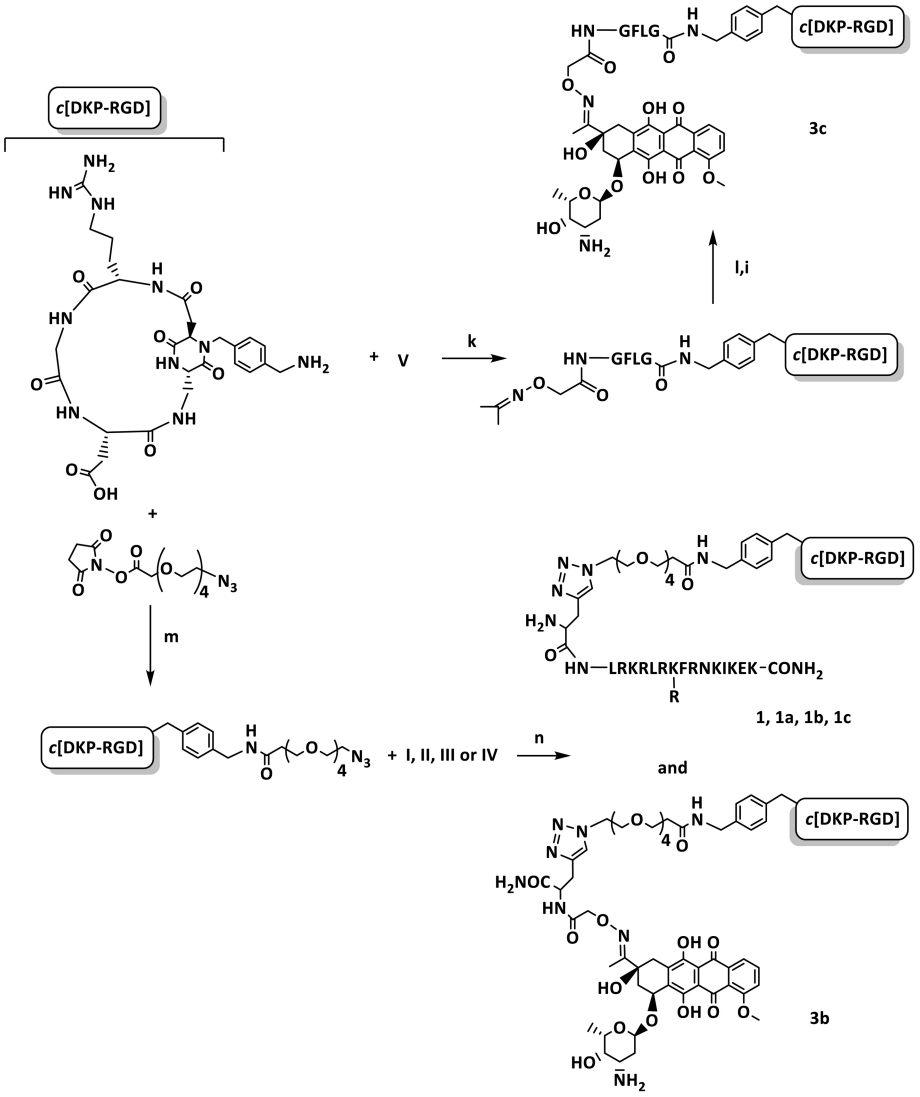

[a]**k**: 5 equiv TSTU, 5 equiv DIPEA, dry DMF, on; **l**: methoxylamine 1 M, NH_4OAc 0.2 M, pH 5; **i** (see Scheme 1); **m**: PBS/MeCN, pH 7.3−7.5, overnight; **n**: 0.5 equiv $CuSO_4 \cdot 5H_2O$, 0.6 equiv Na ascorbate, H_2O:DMF 1:1, 10 mM, 40 °C, N_2, 24 h. (B: propargylglycine).

Table 1. List of All Synthesized Compounds with Their Names, Molecular Weights (MW), and IC_{50} Values

Code	Conjugate	MW [g/mol]	MW_{exp} [g/mol]	IC_{50} [nM] $\alpha_v\beta_3$[a]	IC_{50} [μM] $\alpha_v\beta_5$[a]
1	*c*[DKP-RGD]-sC18	2998.2	2998.3	16.7 ± 0.6	24.9 ± 2.7
1a	*c*[DKP-RGD]-PEG_4-sC18(Lys_8-CF)	3355.9	3356.6	15.3 ± 5.2	2.5 ± 0.2
1b	*c*[DKP-RGD]-PEG_4-sC18(dau=Aoa-Lys_8)	3580.1	3581.1	31.7 ± 4.2	>10
1c	*c*[DKP-RGD]-PEG_4-sC18(dau=Aoa-GFLG-Lys_8)	3954.6	3955.6	9.7 ± 4.0	>10
2	sC18	2069.6	2069.9	n.d.	n.d.
2a	sC18(Lys_8-CF)	2427.9	2428.9	n.d.	n.d.
2b	sC18(dau-Aoa-Lys_8)	2652.2	2653.2	n.d.	n.d.
3a	*c*[DKP-RGD]	630.7	631.3	26.4 ± 3.7[b]	>5[b]
3b	*c*[DKP-RGD]-PEG_4-Aoa=dau	1584.2	1585.0	14.0 ± 1.6	6.3 ± 0.4
3c	dau=Aoa-GFLG-*c*[DKP-RGD]	1587.4	1587.9	5.8 ± 0.6	2.1 ± 0.1

[a]Inhibition of biotinylated vitronectin binding to $\alpha_v\beta_3$ and $\alpha_v\beta_5$ receptors. IC_{50} values were calculated as the concentration of compound required for 50% inhibition of biotinylated vitronectin binding as estimated by GraphPad Prism software; all values are the arithmetic mean SD of triplicate determinations. [b]Ref 50. n.d.: not determined.

peptide carrier as depicted in Schemes 1 and 2. Meanwhile, *c*[DKP-RGD] was prepared as previously described and functionalized with an azido PEG_4-spacer.[49,50] Finally, all CPP precursors where connected with the integrin targeting ligand by CuAAC yielding the novel conjugates **1**, **1a**, **1b**, and **1c** (Scheme 2).

In addition to the drug conjugates containing both the CPP and the integrin ligand, a series based on the CPP alone (**2**, **2a**,

DOI: 10.1021/acs.bioconjchem.9b00292
Bioconjugate Chem. 2019, 30, 2011−2022

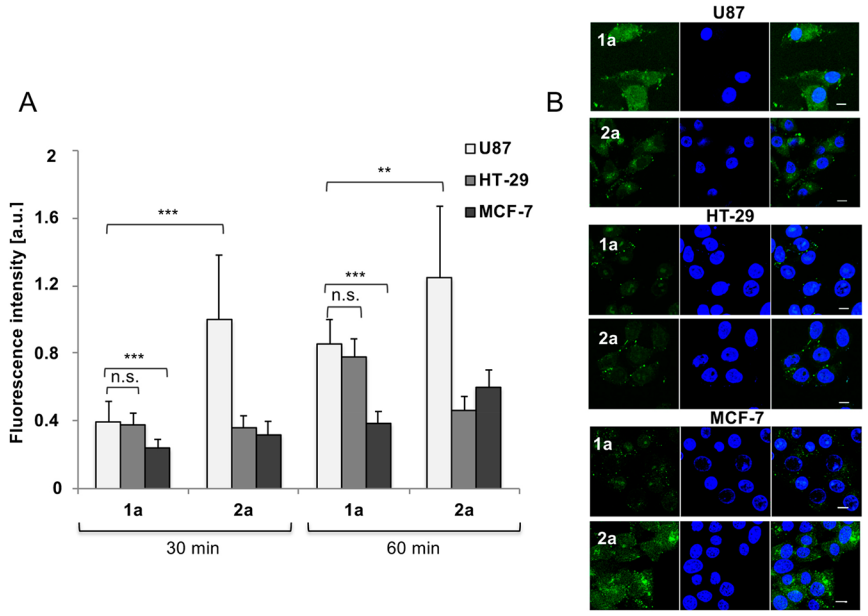

Figure 2. (A) Cellular uptake in U87, HT-29, and MCF-7 cells as quantified by flow cytometry. Cells were incubated with 10 μM of CF-labeled peptide solution for 30 and 60 min at 37 °C. ***: $p < 0.001$; **: $p < 0.005$ (unpaired t test). (B) Cellular uptake was analyzed by confocal laser scanning microscopy. Cells were incubated for 30 min with 10 μM of CF-labeled peptide solution. Green: CF-labeled peptide; blue: Hoechst 33342 nuclear stain; scale bar is 10 μm.

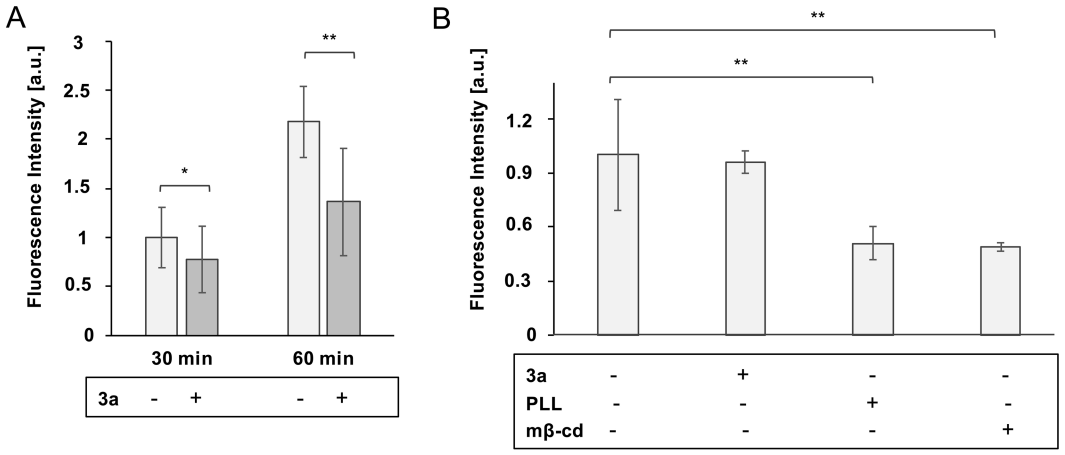

Figure 3. (A) Competition experiment: coincubation of the peptide (10 μM) with compound **3a**, added in excess compared to **1a** (10×). *: $p > 0.5$; **: $p < 0.01$ (unpaired t test). (B) Blocking experiment: 30 min preincubation with **3a** (10 μM) poly(L-lysine) or methyl-β-cyclodextrin (1 mM) followed by 30 min incubation with a solution of **1a** (10 μM). **: $p < 0.02$ (unpaired t test).

and **2b**; refer to Table S1 for sequences), as well as the free integrin ligand (**3**) and the drug-loaded *c*[DKP-RGD] compounds **3b** and **3c** were also considered and prepared (Schemes 1 and 2). All compounds were identified by mass spectrometry and purified by preparative HPLC (Supporting Information).

***In Vitro* Binding Assay on Isolated Integrin Receptors.** In a first instance, we measured the binding affinity of the new conjugates to the isolated integrin receptors $\alpha_v\beta_3$ and $\alpha_v\beta_5$, which are both tumor-associated integrins (Table 1). All compounds tested were able to inhibit biotinylated vitronectin binding to $\alpha_v\beta_3$ with low nanomolar affinity, indicating that the presence of the CPP did not interfere with receptor targeting by the integrin-targeting unit. **3a** was already reported to be up to 200-fold more selective for $\alpha_v\beta_3$ with respect to $\alpha_v\beta_5$.[49,50] Interestingly, herein this selectivity was even more pronounced for the conjugates **1** (up to 1500-fold), **1b** (up to 330-fold), **1c** (up to 1000-fold), as well as conjugates **3b** (up to 420-fold) and **3c** (up to 340-fold).

Cellular Uptake of CF-Labeled Conjugates. For further *in vitro* cell studies we used U87 glioblastoma, MCF-7 breast cancer, and HT-29 colon carcinoma cells. For all of them, we investigated the $\alpha_v\beta_3$ integrin expression by using flow cytometry (Figure S1). U87 cells are reported to have an enhanced expression of integrin $\alpha_v\beta_3$; on the contrary, HT-29 express $\alpha_v\beta_5$ but not $\alpha_v\beta_3$, and therefore they can be used as a negative control.[51] Our data confirmed these expression profiles and did further reveal that also MCF-7 cells expressed $\alpha_v\beta_3$ receptors only to a minor amount, but anyway higher than HT-29 cells.

The cellular uptake of the novel conjugates was then studied in more detail, using the fluorescently labeled conjugates **1a** and **2a**, containing the integrin ligand and the CPP (**1a**) and only the CPP (**2a**), respectively. Cells were incubated with the

DOI: 10.1021/acs.bioconjchem.9b00292
Bioconjugate Chem. 2019, 30, 2011−2022

A

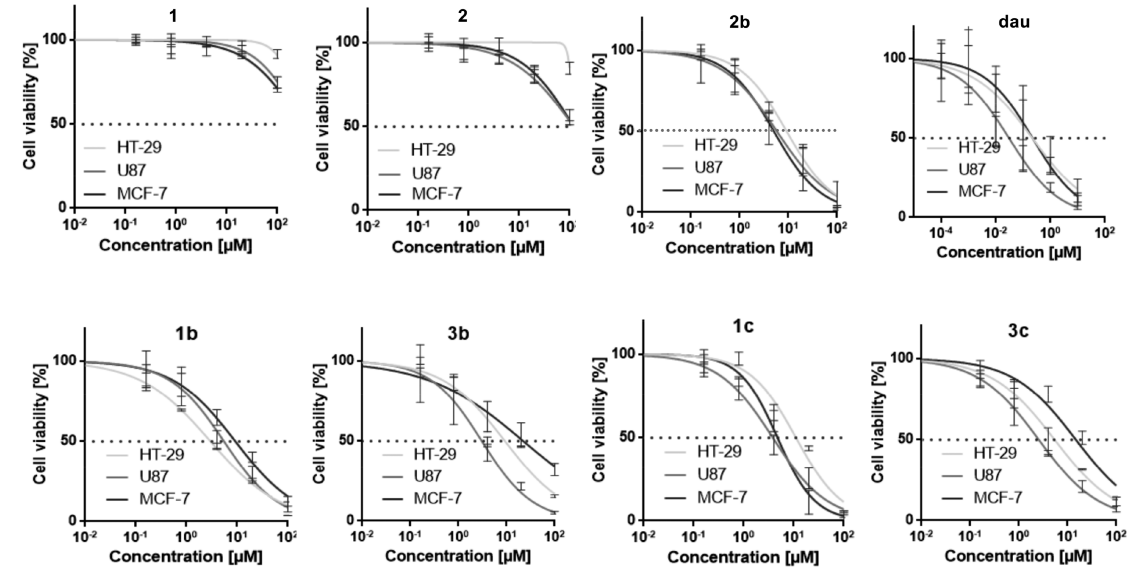

B

	EC_{50}(μM)				
	1b	**2b**	**3b**	**1c**	**3c**
U87	5.6 ± 1.1	5.8 ± 1.5	3.0 ± 0.7	3.9 ± 3.9	2.5 ± 0.7
HT-29	3.0 ± 0.2	9.2 ± 0.1	9.2 ± 0.9	11.0 ± 1.1	5.4 ± 1.3
MCF-7	9.1 ± 2.1	5.0 ± 1.1	21.7 ± 8.3	2.7 ± 0.8	14.7 ± 6.5

Figure 4. Antiproliferative activity of the dau-conjugates, and **1**, **2**, as well as dau alone as controls in human U87, HT-29, and MCF-7 cells after 72 h without washout. (A) shows exemplarily dose−response curves, from which the effective concentrations at which 50% of all cells were dead (EC_{50}) were calculated (B).

compounds at 10 μM concentration at two different time points: 30 and 60 min.

The internalization of **1a** varied significantly over the incubation time in all the three cell lines tested, while this effect was not that obvious for sC18 itself. Interestingly, conjugate **1a** was taken up in U87 and HT-29 cells at nearly the same ratio, while the uptake in MCF-7 cells was significantly lower. Compared to this, conjugate **2a** was internalized in U87 cells much more than in HT-29 or MCF-7 cells. Moreover, the uptake in U87 was much more intensive compared to **1a**, leading to the assumption that the internalization ability was somehow altered by the addition of the targeting unit. An analysis of the intracellular fate was done using confocal fluorescence microscopy and supported the previously obtained data. Both conjugates, **1a** and **2a**, were effectively internalized, but displayed different intracellular distribution patterns: while in HT-29 the compounds are initially entrapped in cytosolic vesicles and then internalized into the nuclei, the distribution in the other two cell lines showed the presence of the peptide conjugates also within the cytoplasm (Figure 2B). All in all, we did not observe any differences in the internalization pattern of **1a** to **2a**, and we were, thus, not able to define the impact of the targeting unit on the entry pathway. To elucidate more precisely this impact, and also, whether integrin receptor-mediated endocytosis was involved, we performed more experiments using U87 cells only.

First, the cellular uptake of **1a** after 30 and 60 min coincubation with the free ligand **3a** was analyzed. The presence of an excess (10-fold molar concentration) of the integrin ligand was expected to compete with the integrin binding sites, thus hampering the internalization of the conjugates. Notably, the uptake of **1a** was only slightly reduced when inspecting the cells after 30 min (Figure 3A). However, this reduction seemed to increase significantly after incubating the cells for a longer time period. This would indicate a cellular uptake mediated by the CPP part of the conjugate and only a minor influence of integrin receptor-mediated endocytosis. We further investigated this effect by blocking the cells by 30 min preincubation with free ligand **3a**, poly(L-lysine) (PLL) or methyl-β-cyclodextrin (mβ-cd) (Figure 3B). Once again, blocking with **3a** had only minor influence, while PLL and mβ-cd significantly reduced the cellular uptake. Poly(L-lysine) occupies all negatively charged groups at the outer surface of the cell membrane, and thus, disturbs CPP-mediated interaction with membrane constituents.[52] Previously, we found out that the presence of cholesterol is not that important for the cellular uptake of sC18 alone in MCF-7 and HEK293 cells.[15] Interestingly, this picture changed for **1a**, which is obviously dependent on the presence of cholesterol, and whose cellular uptake significantly decreased after incubating the cells first with mβ-cd. This might hint to a different uptake pathway compared to the CPP alone. All in all, we concluded that after interfering with the $\alpha_v\beta_3$ receptor, the dual functional conjugate prefers CPP-mediated cellular internalization.

Cytotoxicity of the Peptide−Drug Conjugates. In a next step, the cytotoxic profiles of the dau-coupled conjugates (**1b**, **2b**, **3b**, **1c**, **3c**), as well as the control compounds **1** and **2**, were investigated. All cell lines, U87, HT-29, and MCF-7, were

DOI: 10.1021/acs.bioconjchem.9b00292
Bioconjugate Chem. 2019, 30, 2011−2022

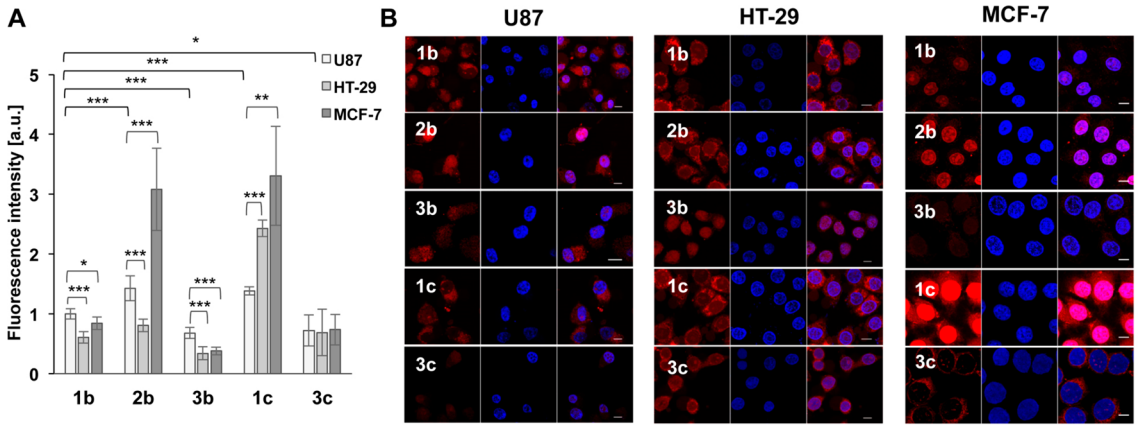

Figure 5. (A) Cellular uptake of the drug-loaded conjugates **1b**−**3b**, **1c**, and **3c** in U87, HT-29, and MCF-7 cells as quantified by flow cytometry. Cells were incubated with 10 μM of peptide solution for 15 min at 37 °C. *: $p < 0.01$; **: $p < 0.001$; ***: $p < 2 \times 10^{-5}$ (unpaired t test). (B) Confocal laser scanning microscopy of U87, HT-29, and MCF-7 cells after incubating them for 30 min with 10 μM of peptide conjugate solutions. Red: dau fluorescence; blue: Hoechst 33342 nuclear stain; scale bar is 10 μm.

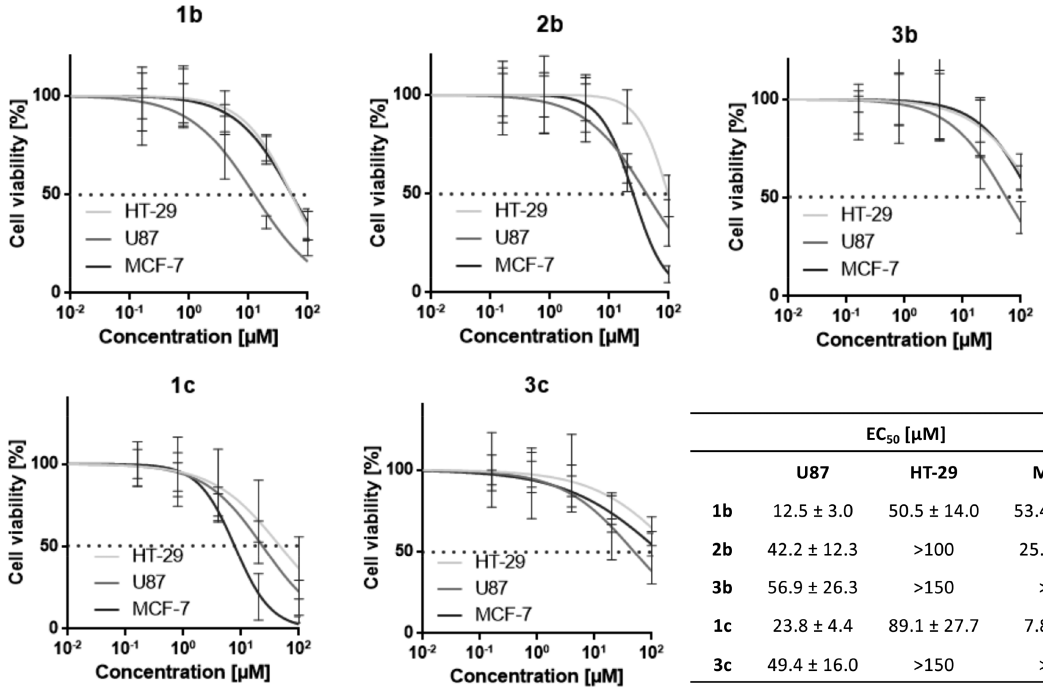

	EC_{50} [μM]		
	U87	HT-29	MCF-7
1b	12.5 ± 3.0	50.5 ± 14.0	53.4 ± 15.6
2b	42.2 ± 12.3	>100	25.1 ± 4.5
3b	56.9 ± 26.3	>150	>150
1c	23.8 ± 4.4	89.1 ± 27.7	7.8 ± 1.5
3c	49.4 ± 16.0	>150	>150

Figure 6. Antiproliferative activity of conjugates **1b**, **2b**, **3b**, **1c**, and **3c** in U87, HT-29, and MCF-7 cells. Cells were incubated for 15 min with peptide solution, and then this solution was removed and cells were incubated for further 72 h. Values from the positive control (DMSO/EtOH; 1:1) were subtracted from all data, and the untreated cells were set to 100%. Exemplary dose−response curves are shown from which the effective concentrations at which 50% of all cells were dead (EC_{50}) were calculated.

incubated for 72 h with different concentrations of the conjugates (Figure 4). Compound **1** showed minor toxicity when applied at 100 μM to U87 and MCF-7 cells, in substantial agreement with the observation that the targeting-unit alone can induce cellular anoikis upon prolonged treatment.[53] The free peptide (**2**) significantly harmed U87 and MCF-7 cells at concentrations of about 100 μM, thus confirming our observation that sC18 can have an impact on cell viability of cancer cells upon treatment with higher concentrations.[16] Both compounds, on the other hand, showed almost no influence on cell viability when applied to HT-29 cells. These results probably directly reflect the outcomes from the cellular uptake analysis, and the observed higher cytotoxic effect against U87 cells is directly proportional with the higher cellular uptake in this cell line.

All dau-loaded conjugates showed high toxicity in all cell lines tested with EC_{50} values in the lower micromolar range (Figure 4). These toxic effects are, however, definitely lower than the nanomolar EC_{50} values shown by free drug daunorubicin, and this effect is possibly due to the release of a daunorubicin derivative, derived from proteolytic cleavage (dau=Aoa-Gly and H-Lys), and of the free drug. Moreover, no clear selectivity trend could be distinguished for the different conjugates among the tested cell lines; compounds **3b** and **3c**, containing only the integrin ligand, showed a moderate selective cytotoxic effect for the integrin expressing cells U87, whereas for conjugate **2b** containing only the CPP, no selectivity at all was observed.

DOI: 10.1021/acs.bioconjchem.9b00292
Bioconjugate Chem. 2019, 30, 2011−2022

Overall, these results suggest a strong influence of the CPP moiety in the internalization of the compounds, as already observed in the uptake studies discussed above.

Investigating the Impact of Short Contact Times on Cellular Uptake and Cytotoxicity. As a means to investigate the possible role of the integrin ligand and the cell-penetrating peptide in the targeting and internalization of our constructs, we chose to incubate the cells for only a very short contact time with the drug-loaded conjugates (15 min). In this manner, we aimed at clarifying whether the establishment of a rapid binding of the integrin targeting moiety to the surface receptor would help increase the selectivity of the constructs, rather than the CPP-driven unspecific uptake observed in the long incubation (72 h) experiments. This procedure would also better simulate *in vivo* conditions, in which the administered drug is assumedly rapidly cleared from the tumor extracellular environment.

The cellular uptake of the dau-loaded conjugates was first evaluated by flow cytometry after 15 min of incubation: all the compounds were internalized, albeit to different extents (Figure 5A).

In particular, compounds **3b** and **3c**, possessing the integrin targeting moiety and devoid of the CPP were internalized with reduced efficiency: **3b** was taken up in the lowest amounts although with a significant preference for U87 compared to HT-29 and MCF-7 cells, while **3c**, containing the cathepsin B cleavage sequence showed similar internalization and no preference for any particular cell line. This observation confirms the reduced internalization of integrin ligand drug conjugates cited above. On the other hand, sC18-dau (**2b**), internalized most in MCF-7, followed by U87 and HT-29. This internalization ability is different than the one displayed by **2a**, i.e., the CF-labeled CPP, and this can be explained by the different physicochemical properties of CF with respect to dau. A significant preference for U87 cells was displayed by conjugate **1b**, bearing the integrin targeting ligand and the CPP but not the cathepsin cleavable linker. In this case, the internalization profile matched the integrin expression found for the three cell lines. Interestingly, this effect was reversed for **1c**: in this case, the uptake in U87 was lower compared to HT-29 and MCF-7 cells, in which **1c** internalized to very high extents. With these studies, it became clear that the novel conjugates need only very short contact times to internalize into the cells. Moreover, it seemed that introducing a cathepsin B cleavage site led on one hand to improved activity, but on the other hand lowered selectivity of the conjugates.

Finally, we investigated how these short contact times would impact cell viability of the different cell lines. Therefore, cells were incubated with the compound solutions only for 15 min, drained, and after addition of fresh cell culture media, cells were incubated for further 72 h. As a general comment, the cytotoxicity measured by this methodology parallels the internalization ability of the same compounds, obtained with the same 15 min incubation time. More specifically, compounds **1b** and **3b** demonstrated significantly higher activity against U87 cells compared to MCF-7 and HT-29 cells (Figure 6). Importantly, **1b** was more active than **3b** demonstrating that the attached CPP is indeed necessary to increase the overall cellular uptake and thus cytotoxic activity of the conjugates. Of note is also that **2b** was less efficient than **1b** but marginally more active than **3b**, although with no selectivity. For the two conjugates bearing the GFLG motif, it was seen that **3c** is still significantly more active in U87 cells expressing integrin receptors. By contrast, **1c** kept its selectivity against HT-29 cells, but was pronouncedly more active in MCF-7 cells compared to **1b**. This is presumably due to the reasons discussed before, and mainly based on higher amounts of cathepsin B in MCF-7 cells.

CONCLUSION

Summarizing, we present here for the first time peptide−drug conjugates composed of a diketopiperazine-based integrin-targeting unit and a cell-penetrating peptide. The synthesis is very straightforward and allows incorporation of different active groups, like the fluorescent dye CF, or the drug daunorubicin, which were coupled to the CPP via a lysine side chain. We found out that the cellular uptake follows a "kiss-and-run"-like model, in which internalization is mediated mainly by the CPP part, while the targeting unit helps to direct the conjugates selectively to $\alpha_v\beta_3$ integrin-expressing cells. Based on only the short contact times needed for selective targeting of integrin-expressing cells, these novel PDCs are highly valuable and promising compounds for the further development of anticancer drugs. Moreover, the association of the targeting unit and the CPP proved to be a necessary and powerful link that is worth studying in more detail, also by including other, possibly more cytotoxic, payloads. In the future, we aim to use *in vivo* models for investigating the selectivity of these novel PDCs against $\alpha_v\beta_3$ overexpressing tumoral cells. Furthermore, the combination of these conjugates with nanoparticle formulations could lead to the formation of interesting multimodal drug delivery systems with tremendous impact in this context. Recently, significant progress in this direction has been demonstrated.[31] Hopefully, with these further studies, we will provide a new perspective on the development of targeted CPP-based drug delivery systems.

EXPERIMENTAL SECTION

Material. Nα-Fmoc-protected amino acids, Oxyma Pure, diisopropylcarbodiimide (DIC), trifluoroacetic acid, and 4-(2′,4′-dimethoxyphenyl-Fmoc-aminomethyl)phenoxy (Rink amide) resin were purchased from IRIS Biotech GmbH (Marktredwitz, Germany). The following side chain protecting groups were used: 2,2,4,6,7-pentamethyldihydrobenzofuran-5-sulfonyl (Pbf) for Arg; Trityl (Trt) for Asn, His, and Gln; *tert*-Butyl (*t*Bu) for Asp and Glu; *tert*-butyloxycarbonyl (Boc) for Lys. For the selective deprotection of side chains also Fmoc-Lys(Dde)-OH was used. Unless otherwise stated, all reagents, solvents, and consumables used were purchased from the companies Alfa Aesar (Karlsruhe, Germany), Greiner Bio-One (Kremsmünster, Austria), IRIS Biotech GmbH (Marktredwitz, Germany), LP Italiana SPA (Milano, Italy), Merck (Darmstadt, Germany), Roth (Karlsruhe, Germany), Ratiolab GmBH (Dreieich, Germany), Sigma-Aldrich (Taufkirchen, Germany), Sarstedt (Nümbrecht, Germany), and VWR BDH Prolabo (Darmstadt, Germany), and their purity fulfilled at least the specifications for synthesis quality. Daunorubicin hydrochloride was a gift from Prof. Dr. Gábor Mező (Budapest, Hungary).

Methods. *Synthesis of the Drug-Free Conjugates.* Peptides were synthesized on Rink amide resin (100−200 mesh, loading: 0.48 mmol/g) by automated solid-phase peptide synthesis (SPPS) on a multiple Syro II peptide synthesizer (Multi-SynTech, Witten, Germany). Fmoc/*t*Bu-strategy using a double-coupling procedure and *in situ* activation with Oxyma/DIC was used. Fmoc-Lys(Dde)−OH, propargylglycine, and 5,6-carboxyfluorescein (CF) were coupled manually to the peptides using 3 equiv of the reagent, 3 equiv Oxyma, and 3 equiv DIC for

DOI: 10.1021/acs.bioconjchem.9b00292
Bioconjugate Chem. 2019, 30, 2011−2022

2 h or overnight; the procedure was repeated twice. The success of the coupling was then controlled by Kaiser test. For the labeling with CF the N-terminus was protected with a Boc group by a reaction with 10 equiv di-*tert*-butyl-dicarbonate and 1 equiv DIPEA in DCM for 2 h. After that, Dde cleavage was performed with a solution of 3% hydrazine in DMF (12 × 10 min). The peptide was finally cleaved from the resin using TFA:water:TIS (95:2.5:2.5, v/v/v). After 3 h reaction at room temperature, the peptides were precipitated in ice cold diethyl ether and then washed and centrifuged 5 times at 4 °C, 5000 rpm; the pellet was lyophilized from water:*tert*-butyl alcohol (3:1 v/v) and analyzed by RP-HPLC-ESI-MS on a Chromolith Performance RP-18e column, 100 × 4.6 mm from Merck (Darmstadt, Germany), and using linear gradients of 10−60% B in A (A = 0.1% FA in water; B = 0.1% FA in acetonitrile) over 15 min and a flow rate of 0.6 mL min^{-1}. Further purification of the peptides was achieved by preparative HPLC, Hitachi Elite LaChrom (VWR, Darmstadt, Germany) on RP18 column Nucleodur C18ec, 100−5 from Macherey-Nagel (Düren, Germany) at 6 mL min^{-1} and 220 nm detection. Acetonitrile/water with 0.1% TFA were used as eluents, changing gradient as needed. The collected fractions were evaporated, analyzed with LC-MS, and lyophilized to obtain the purified peptides with purities >95%.

Coupling of the Peptide to the c[DKP-RGD]-PEG_4-N_3. The c[DKP-RGD]-PEG_4-N_3 was conjugated to the peptide conjugate by a copper(I) catalyzed azide−alkyne cycloaddition (click reaction) occurring between the azido group of the PEG linker and the alkyne group of the propargylglycine. 1.3 equiv of the azido compound was dissolved with 1 equiv of the alkyne-containing peptide in dry DMF/degassed water 1:1 in a Schlenk tube under nitrogen atmosphere reaching a concentration of 10 mM. Stock solutions of $CuSO_4$ and Na ascorbate in degassed water were prepared and 0.5 equiv and 0.6 equiv, respectively, were added to the reaction. The solution was stirred overnight under nitrogen atmosphere at 40 °C. The reaction was followed by LC-MS to completion and then directly injected into the HPLC on a semipreparative RP18 column for purification obtaining final conjugates with purities >95%.

Synthesis of the Drug Conjugates Containing the CPP Moiety. The synthesis of the peptide followed the same procedure as previously described. For the attachment of the daunorubicin to the peptide by an oxyme bond, a molecule of Bis-Boc aminooxyacetic acid was coupled to the side chain of a lysine (3 equiv with oxyma and DIC overnight). The success of the coupling was checked by Kaiser test. The cleavage from the resin occurred with the standard scavenger, but, as already described by Mezö et al.,[54] 10 equiv of Boc-aminooxyacetic acid was added in the cleavage cocktail in order to avoid the formation of the aceton adduct with mass +40. After precipitation, washing, and purification, the peptide was dissolved in ammonium acetate buffer 0.2 M at pH 5 reaching a concentration of 10 mg peptide/mL for the coupling to the drug. Daunorubicin was added in excess of about 30% and the reaction was stirred overnight. In order to remove excess of daunorubicin, the reaction solution was directly injected into the HPLC on a semipreparative RP18 column Nucleodur C18ec, 100−5 from Macherey-Nagel (Düren, Germany) at 1.5 mL min^{-1} and 220 nm detection. Acetonitrile/water with 0.1% TFA were used as eluents, changing gradient as needed. The collected fractions were evaporated, analyzed with LC-MS, and lyophilized to obtain the purified peptides with purities >95%.

*Synthesis of Compound **3b**.* Rink amide resin (144 μmol scale) was manually loaded with the Fmoc-propargylglycine−OH (oxyma, DIC, overnight and HATU, DIPEA for 2 h). After a capping procedure to block the unreacted groups on the resin (acetic anhydride and DIPEA in DMF), Fmoc deprotection of the amino acid with 30% solution of piperidine in DMF was performed. Bis-Boc-Aminooxyacetic acid was then manually coupled twice (Oxyma, DIC in DMF for 2 h). Full cleavage of the peptide from the resin was performed using TFA:TIS:water (90:2.5:2.5, v/v/v) in the presence of 5 equiv Boc-Aoa−OH. The dipeptide was precipitated in ice cold diethyl ether/hexane 1:3 and then washed, lyophilized, and purified. Further steps followed the same strategy as previously described.

*Synthesis of **3c**.* The GLFG tetrapeptide was synthesized on a 2-chlorotrityl chloride resin (H-Gly-2CT Resin, 100−200 mesh, 0.87 mmol/g, 0.015 mmol scale) by automated multiple solid-phase peptide synthesis (Fmoc strategy). Bis-Boc-Aminooxy-acetic acid was coupled manually. After cleavage from the resin, the peptide was purified by HPLC and then stirred in acetone for 30 min at room temperature to protect the aminooxy group with an isopropylidene group. c[DKP-RGD] was then coupled to the C-terminus of the peptide using TSTU and DIPEA (both 5 equiv) in dry DMF (20 mM). The reaction was incubated overnight and then directly purified by HPLC. The isopropylidene group was then cleaved from the Aoa dissolving the peptide in 1 M CH_3ONH_2·HCl (methoxylamine hydrochloride) containing NH_4OAc-buffer (0.2 M, pH 5) (20 equiv at least). The reaction mixture was then directly purified by semipreparative HPLC. Finally, dau (30% excess) was coupled to the deprotected aminooxyacetylated peptide, as previously described, yielding conjugate **3c** in satisfactory yield after HPLC purification (60%).

Solid-Phase Receptor Binding Assay. Human integrin receptors $\alpha_v\beta_3$ (R&D Systems, Minneapolis, MN, USA) and $\alpha_v\beta_5$ (EMD Millipore Corporation, Inc., Temecula, CA, USA) were diluted to 0.5 μg/mL in coating buffer containing 20 mM Tris-HCl (pH 7.4), 150 mM NaCl, 1 mM $MnCl_2$, 2 mM $CaCl_2$, and 1 mM $MgCl_2$. An aliquot of diluted receptor (100 μL/well) was added to 96-well microtiter plates (Nunc MaxiSorp, Termo Fisher Scientific, Roskilde, DK) and incubated overnight at 4 °C. The plates were incubated with blocking solution (coating buffer plus 1% bovine serum albumin) for additional 2 h at room temperature to block nonspecific binding. After washing 2 times with blocking solution, plates were incubated shaking in the dark for 3 h at room temperature, with various concentrations (10^{-5}−10^{-12} M) of test compounds in the presence of 1 μg/mL vitronectin (Molecular Innovations, Novi, MI, USA) biotinylated using an EZ-Link Sulfo-NHS-Biotinylation kit (Pierce, Rockford, IL, USA). After washing 3 times, the plates were incubated shaking for 1 h in the dark, at room temperature, with streptavidin−biotinylated peroxidase complex (Amersham Biosciences, Uppsala, Sweden). After washing 3 times with blocking solution, plates were incubated with 100 μL/well of Substrate Reagent Solution (R&D Systems, Minneapolis, MN, USA) for 30 min shaking in the dark, before stopping the reaction with the addition of 50 μL/well 2 N H_2SO_4. Absorbance at 415 nm was read in a Synergy HT Multi-Detection Microplate Reader (BioTek Instruments, Inc.). Each data point represents the average of triplicate wells; data analysis was carried out by nonlinear regression analysis with GraphPad Prism software. Each experiment was repeated in duplicate.

Cell Culture. All the cell experiments were carried out under a laminar flow hood Herasafe. The temperature (37 °C) of the chemicals used was adjusted by Julabo SW22 heating bath. Cell culture was carried out at 5% CO_2 at 37 °C, using 100 × 20 mm

DOI: 10.1021/acs.bioconjchem.9b00292
Bioconjugate Chem. 2019, 30, 2011−2022

Petri dishes. The medium used for the U87 cells was Dulbecco's Modified Eagle's Medium, high glucose, supplemented with 10% fetal bovine serum (FBS) and 2 mM L-Glutamine and for the MCF-7 and HT-29 cells RPMI medium (90%) with FBS (10%) and 2 mM L-glutamine. For cell culturing Dulbecco's phosphate buffered saline (PBS 1×) and trypsin-EDTA solution have been used. All these reagents were obtained from Sigma-Aldrich (Taufkirchen, Germany). MTT (3-(4,5-dimethylthiazol-2-yl)-2,5-diphenyl-tetrazolium bromide) was obtained from Acros Organics (Geel, Belgium).

Integrin Expression on Cell Surface. Three million cells were counted for every cell line, then centrifuged in 15 mL tubes at 1,000 rpm for 5 min at 4 °C; afterwards, the supernatant was removed. To fix the cells, 300 μL of 4% paraformaldehyde was added to the pellet, which was then resuspended and left 10 min at rt. Afterward, 2 mL of PBS was added, and the 15 mL tubes vortexed and centrifuged at 1,000 rpm, 5 min at 4 °C. The supernatant was discarded and 3 mL PBS was added to the 15 mL tubes. The solution was again resuspended and divided into 3 FACS tubes (one as control and two for the treatment with antibody). The antibody used was an anti-integrin $\alpha_v\beta_3$ Ab clone LM609 purchased from Merck Millipore. After addition of 2 mL of PBS to each tube, centrifugation followed with the same conditions as before and supernatant was removed. 50 μL of 3% BSA in PBS was added to each tube to block nonspecific binding sites. The solution was left for 10 min at rt and moved from time to time. After this blocking step, 50 μL of antibody mixture (dilution 1:25; 2 μL antibody, 23 μL PBS, and 25 μL 3% BSA) were added to each FACS tube, incubated for 60 min at 37 °C, and moved from time to time. After this incubation time, cells were washed by adding 2 mL of PBS. Centrifugation was performed, the supernatant removed, and the pellet was then dissolved in FACS medium to proceed with the quantification of the fluorescence intensity.

MTT Cytotoxicity Assay. To investigate the antiproliferative activity of the conjugates on the human tumor cell lines U87, HT-29 and MCF-7, a MTT assay was performed. Cells were seeded in a 96-well plate purchased from Greiner Bio-One (Frickenhausen, Germany) (6,000 cells per well), grown for 24 h, and incubated with various concentrations of the conjugate in appropriate serum-containing medium for 72 h or 15 min, followed by medium removal, and incubation with fresh medium for additional 72 h under standard growth conditions. The MTT assay was performed by adding 20 μL of MTT solution (5 mg mL^{-1} in PBS) to each well and after 3 h of incubation at 37 °C, the supernatant was removed. The formazan crystals were dissolved in 100 μL of a 1:1 solution of DMSO and EtOH and the absorbance was determined at 570 nm with a microplate reader (BIO-RAD, model 550). Background value (absorbance of DMSO−EtOH) was subtracted from the measured values and the percentage decrease in cell proliferation was determined relatively to untreated cells.

Quantification of Cellular Uptake and Competition/Blocking Experiment by Flow Cytometry. For uptake studies by flow cytometry, cells were seeded in a 24-well plate (U87: 150,000 cells per well; HT-29 and MCF-7:120,000 cells per well) and grown to 70−80% confluency. After incubation at 37 °C for 15, 30, or 60 min with the labeled peptides (CF or daunorubicin) in serum-free medium, the cells were washed twice with PBS, detached with indicator-free trypsin and resuspended in indicator-free serum containing-RPMI medium. The cell suspension was moved into a 96-well FACS plate and the fluorescence was then measured by a Guava easyCyte flow cytometer (Merck) where 10,000 viable cells were counted. Cellular autofluorescence was subtracted. The experiments were performed twice in triplicates. For competition experiment the unfunctionalized c[DKP-RGD] ligand was added in 10-fold excess together with the peptide. After 30 or 60 min incubation time the medium was removed and the cells were treated as described above. For blocking experiments, the cells were preincubated with *c*[DKP-RGD] (10 μM), poly(L-lysine) or methyl-β-cyclodextrin (1 mM) for 30 min and then treated with the peptide for 30 min.

Microscopy Studies for Cellular Uptake. For confocal microscopy uptake studies, cells were seeded in an eight-well (Ibidi) plate (U87:70,000 cells per well; HT-29 and MCF-7:50,000 cells per well), and grown to 70−80% confluency. The cells were then incubated with CF- or daunorubicin-labeled peptides in serum-free medium for 30 min at 37 °C. The nuclei were stained for 10 min with Hoechst 33342 nuclear dye (bisbenzimide H33342, 1 mg/mL in H_2O, sterile filtered) prior to the end of peptide incubation. Finally, the solution was removed and cells were treated with 200 μL trypan blue solution (150 mm in 0.1 M acetate buffer, pH 4.15) for 15 s. After washing once with serum-free medium and adding fresh, appropriate serum-containing medium, images were taken by using a Leica SP8 confocal laser scanning microscope equipped with a 60 V oil-immersion objective. Images were recorded with Leica Microsystems software and adjusted equally with Fiji software.

■ ASSOCIATED CONTENT

Supporting Information

The Supporting Information is available free of charge on the ACS Publications website at DOI: 10.1021/acs.bioconjchem.9b00292.

Amino acid sequences of all compounds, analysis of $\alpha_v\beta_3$ expression level, LC-MS data of compounds **1**, **1a**-**1c**, and **2a**-**2b**, **3b**, **3c** (PDF)

■ AUTHOR INFORMATION

Corresponding Authors

*E-mail: umberto.piarulli@uninsubria.it.
*E-mail: ines.neundorf@uni-koeln.de.

ORCID

Ines Neundorf: 0000-0001-6450-3991

Notes

The authors declare no competing financial interest.

■ ACKNOWLEDGMENTS

Financing by the European Union within the MSCA-ITN-2014-ETN MAGICBULLET (grant agreement number 642004) is kindly acknowledged by I.N., L.F., U.P., S.P., and C.R. L. Feni thanks I. Randelovic and A. Klimpel for help in cell culture, and preparing the figures. We acknowledge the CECAD Imaging Facility of University of Cologne for assistance with the generation of microscopy data.

■ REFERENCES

(1) Drilon, A., Laetsch, T. W., Kummar, S., DuBois, S. G., Lassen, U. N., Demetri, G. D., Nathenson, M., Doebele, R. C., Farago, A. F., Pappo, A. S., et al. (2018) Efficacy of Larotrectinib in TRK Fusion-Positive Cancers in Adults and Children. *N. Engl. J. Med. 378*, 731−739.

DOI: 10.1021/acs.bioconjchem.9b00292
Bioconjugate Chem. 2019, 30, 2011−2022

(2) Blackhall, F. H., Rehman, S., and Thatcher, N. (2005) Erlotinib in non-small cell lung cancer: a review. *Expert Opin. Pharmacother. 6*, 995−1002.
(3) Schuler, M., Wu, Y. L., Hirsh, V., O'Byrne, K., Yamamoto, N., Mok, T., Popat, S., Sequist, L. V., Massey, D., Zazulina, V., et al. (2016) First-Line Afatinib versus Chemotherapy in Patients with Non-Small Cell Lung Cancer and Common Epidermal Growth Factor Receptor Gene Mutations and Brain Metastases. *J. Thorac. Oncol. 11*, 380−90.
(4) Gadgeel, S. M. (2018) The use of alectinib in the first-line treatment of anaplastic lymphoma kinase-positive non-small-cell lung cancer. *Future Oncol. 14*, 1875−1882.
(5) Tiller, K. E., and Tessier, P. M. (2015) Advances in Antibody Design. *Annu. Rev. Biomed. Eng. 17*, 191−216.
(6) Khoja, L., Butler, M. O., Kang, S. P., Ebbinghaus, S., and Joshua, A. M. (2015) Pembrolizumab. *J. Immunother Cancer 3*, 36.
(7) Hellmann, M. D., Ciuleanu, T. E., Pluzanski, A., Lee, J. S., Otterson, G. A., Audigier-Valette, C., Minenza, E., Linardou, H., Burgers, S., Salman, P., et al. (2018) Nivolumab plus Ipilimumab in Lung Cancer with a High Tumor Mutational Burden. *N. Engl. J. Med. 378*, 2093−2104.
(8) Dine, J., Gordon, R., Shames, Y., Kasler, M. K., and Barton-Burke, M. (2017) Immune Checkpoint Inhibitors: An Innovation in Immunotherapy for the Treatment and Management of Patients with Cancer. *Asia Pac J. Oncol Nurs 4*, 127−135.
(9) Perica, K., Varela, J. C., Oelke, M., and Schneck, J. (2015) Adoptive T cell immunotherapy for cancer. *Rambam Maimonides Med. J. 6*, e0004.
(10) Khoury, J. D., and Catenacci, D. V. (2015) Next-generation companion diagnostics: promises, challenges, and solutions. *Arch. Pathol. Lab. Med. 139*, 11−3.
(11) Naghavi, M. (2017) Global, regional, and national age-sex specific mortality for 264 causes of death, 1980−2016: a systematic analysis for the Global Burden of Disease Study 2016. *Lancet 390*, 1151−1210.
(12) Liu, X., Wu, F., Ji, Y., and Yin, L. (2019) Recent Advances in Anticancer Protein/Peptide Delivery. *Bioconjugate Chem. 30*, 305−324.
(13) Feni, L., and Neundorf, I. (2017) The Current Role of Cell-Penetrating Peptides in Cancer Therapy. *Adv. Exp. Med. Biol. 1030*, 279−295.
(14) Kalafatovic, D., and Giralt, E. (2017) Cell-Penetrating Peptides: Design Strategies beyond Primary Structure and Amphipathicity. *Molecules 22*, 1929.
(15) Schach, D. K., Rock, W., Franz, J., Bonn, M., Parekh, S. H., and Weidner, T. (2015) Reversible Activation of a Cell-Penetrating Peptide in a Membrane Environment. *J. Am. Chem. Soc. 137*, 12199−12202.
(16) Gronewold, A., Horn, M., Randelovic, I., Tovari, J., Munoz Vazquez, S., Schomacker, K., and Neundorf, I. (2017) Characterization of a Cell-Penetrating Peptide with Potential Anticancer Activity. *ChemMedChem 12*, 42−49.
(17) van Lith, S. A. M., van den Brand, D., Wallbrecher, R., van Duijnhoven, S. M. J., Brock, R., and Leenders, W. P. J. (2017) A Conjugate of an Anti-Epidermal Growth Factor Receptor (EGFR) VHH and a Cell-Penetrating Peptide Drives Receptor Internalization and Blocks EGFR Activation. *ChemBioChem 18*, 2390−2394.
(18) Diamantis, N., and Banerji, U. (2016) Antibody-drug conjugates–an emerging class of cancer treatment. *Br. J. Cancer 114*, 362−7.
(19) Hedrich, W. D., Fandy, T. E., Ashour, H. M., Wang, H., and Hassan, H. E. (2018) Antibody-Drug Conjugates: Pharmacokinetic/Pharmacodynamic Modeling, Preclinical Characterization, Clinical Studies, and Lessons Learned. *Clin. Pharmacokinet. 57*, 687−703.
(20) Garcia-Alonso, S., Ocana, A., and Pandiella, A. (2018) Resistance to Antibody-Drug Conjugates. *Cancer Res. 78*, 2159−2165.
(21) Cazzamalli, S., Dal Corso, A., Widmayer, F., and Neri, D. (2018) Chemically Defined Antibody- and Small Molecule-Drug Conjugates for in Vivo Tumor Targeting Applications: A Comparative Analysis. *J. Am. Chem. Soc. 140*, 1617−1621.
(22) Casi, G., and Neri, D. (2015) Antibody-Drug Conjugates and Small Molecule-Drug Conjugates: Opportunities and Challenges for the Development of Selective Anticancer Cytotoxic Agents. *J. Med. Chem. 58*, 8751−61.
(23) Ma, L., Wang, C., He, Z., Cheng, B., Zheng, L., and Huang, K. (2017) Peptide-Drug Conjugate: A Novel Drug Design Approach. *Curr. Med. Chem. 24*, 3373−3396.
(24) Hatley, R. J. D., Macdonald, S. J. F., Slack, R. J., Le, J., Ludbrook, S. B., and Lukey, P. T. (2018) An alpha v-RGD Integrin Inhibitor Toolbox: Drug Discovery Insight, Challenges and Opportunities. *Angew. Chem., Int. Ed. 57*, 3298−3321.
(25) Hamidi, H., and Ivaska, J. (2018) Every step of the way: integrins in cancer progression and metastasis. *Nat. Rev. Cancer 18*, 532−547.
(26) Nieberler, M., Reuning, U., Reichart, F., Notni, J., Wester, H. J., Schwaiger, M., Weinmuller, M., Rader, A., Steiger, K., and Kessler, H. (2017) Exploring the Role of RGD-Recognizing Integrins in Cancer. *Cancers 9*, 116.
(27) Hatley, R. J. D., Macdonald, S. J. F., Slack, R. J., Le, J., Ludbrook, S. B., and Lukey, P. T. (2018) An alphav-RGD Integrin Inhibitor Toolbox: Drug Discovery Insight, Challenges and Opportunities. *Angew. Chem., Int. Ed. 57*, 3298−3321.
(28) Kapp, T. G., Rechenmacher, F., Neubauer, S., Maltsev, O. V., Cavalcanti-Adam, E. A., Zarka, R., Reuning, U., Notni, J., Wester, H. J., Mas-Moruno, C., et al. (2017) A Comprehensive Evaluation of the Activity and Selectivity Profile of Ligands for RGD-binding Integrins. *Sci. Rep. 7*, 39805.
(29) Katsamakas, S., Chatzisideri, T., Thysiadis, S., and Sarli, V. (2017) RGD-mediated delivery of small-molecule drugs. *Future Med. Chem. 9*, 579−604.
(30) Dal Corso, A., Pignataro, L., Belvisi, L., and Gennari, C. (2015) alpha(v)beta(3) Integrin-Targeted Peptide/Peptidomimetic-Drug Conjugates: In-Depth Analysis of the Linker Technology. *Curr. Top. Med. Chem. 16*, 314−329.
(31) Mansur, A. A. P., Carvalho, S. M., Lobato, Z. I. P., Leite, M. F., Cunha, A. D. S., Jr., and Mansur, H. S. (2018) Design and Development of Polysaccharide-Doxorubicin-Peptide Bioconjugates for Dual Synergistic Effects of Integrin-Targeted and Cell-Penetrating Peptides for Cancer Chemotherapy. *Bioconjugate Chem. 29*, 1973−2000.
(32) Pina, A., Dal Corso, A., Caruso, M., Belvisi, L., Arosio, D., Zanella, S., Gasparri, F., Albanese, C., Cucchi, U., Fraietta, I., et al. (2017) Targeting Integrin alpha(V)beta(3) with Theranostic RGD-Camptothecin Conjugates Bearing a Disulfide Linker: Biological Evaluation Reveals a Complex Scenario. *Chemistryselect 2*, 4759−4766.
(33) Moncelet, D., Bouchaud, V., Mellet, P., Ribot, E., Miraux, S., Franconi, J. M., and Voisin, P. (2013) Cellular density effect on RGD ligand internalization in glioblastoma for MRI application. *PLoS One 8*, e82777.
(34) Cressman, S., Sun, Y., Maxwell, E. J., Fang, N., Chen, D. D. Y., and Cullis, P. R. (2009) Binding and Uptake of RGD-Containing Ligands to Cellular alpha(v)beta(3) Integrins. *Int. J. Pept. Res. Ther. 15*, 49−59.
(35) Sancey, L., Garanger, E., Foillard, S., Schoehn, G., Hurbin, A., Albiges-Rizo, C., Boturyn, D., Souchier, C., Grichine, A., Dumy, P., et al. (2009) Clustering and internalization of integrin alphavbeta3 with a tetrameric RGD-synthetic peptide. *Mol. Ther. 17*, 837−43.
(36) Temming, K., Schiffelers, R. M., Molema, G., and Kok, R. J. (2005) RGD-based strategies for selective delivery of therapeutics and imaging agents to the tumour vasculature. *Drug Resist. Updates 8*, 381−402.
(37) Neundorf, I., Rennert, R., Hoyer, J., Schramm, F., Lobner, K., Kitanovic, I., and Wolfl, S. (2009) Fusion of a Short HA2-Derived Peptide Sequence to Cell-Penetrating Peptides Improves Cytosolic Uptake, but Enhances Cytotoxic Activity. *Pharmaceuticals 2*, 49−65.
(38) da Ressurreicao, A. S., Vidu, A., Civera, M., Belvisi, L., Potenza, D., Manzoni, L., Ongeri, S., Gennari, C., and Piarulli, U. (2009) Cyclic RGD-peptidomimetics containing bifunctional diketopiperazine scaffolds as new potent integrin ligands. *Chem. - Eur. J. 15*, 12184−8.
(39) Marchini, M., Mingozzi, M., Colombo, R., Guzzetti, I., Belvisi, L., Vasile, F., Potenza, D., Piarulli, U., Arosio, D., and Gennari, C. (2012) Cyclic RGD peptidomimetics containing bifunctional diketopiperazine scaffolds as new potent integrin ligands. *Chem. - Eur. J. 18*, 6195−207.

DOI: 10.1021/acs.bioconjchem.9b00292
Bioconjugate Chem. 2019, 30, 2011−2022

(40) McGowan, J. V., Chung, R., Maulik, A., Piotrowska, I., Walker, J. M., and Yellon, D. M. (2017) Anthracycline Chemotherapy and Cardiotoxicity. *Cardiovasc. Drugs Ther. 31*, 63−75.
(41) Vrettos, E. I., Mezo, G., and Tzakos, A. G. (2018) On the design principles of peptide-drug conjugates for targeted drug delivery to the malignant tumor site. *Beilstein J. Org. Chem. 14*, 930−954.
(42) Sapra, P., Stein, R., Pickett, J., Qu, Z., Govindan, S. V., Cardillo, T. M., Hansen, H. J., Horak, I. D., Griffiths, G. L., and Goldenberg, D. M. (2005) Anti-CD74 antibody-doxorubicin conjugate, IMMU-110, in a human multiple myeloma xenograft and in monkeys. *Clin. Cancer Res. 11*, 5257−64.
(43) Horn, M., Reichart, F., Natividad-Tietz, S., Diaz, D., and Neundorf, I. (2016) Tuning the properties of a novel short cell-penetrating peptide by intramolecular cyclization with a triazole bridge. *Chem. Commun. (Cambridge, U. K.) 52*, 2261−4.
(44) Reichart, F., Horn, M., and Neundorf, I. (2016) Cyclization of a cell-penetrating peptide via click-chemistry increases proteolytic resistance and improves drug delivery. *J. Pept. Sci. 22*, 421−6.
(45) Raposo Moreira Dias, A., Pina, A., Dal Corso, A., Arosio, D., Belvisi, L., Pignataro, L., Caruso, M., and Gennari, C. (2017) Multivalency Increases the Binding Strength of RGD Peptidomimetic-Paclitaxel Conjugates to Integrin alphaV beta3. *Chem. - Eur. J. 23*, 14410−14415.
(46) Manea, M., Leurs, U., Orban, E., Baranyai, Z., Ohlschlager, P., Marquardt, A., Schulcz, A., Tejeda, M., Kapuvari, B., Tovari, J., et al. (2011) Enhanced enzymatic stability and antitumor activity of daunorubicin-GnRH-III bioconjugates modified in position 4. *Bioconjugate Chem. 22*, 1320−9.
(47) Mezo, G., and Manea, M. (2010) Receptor-mediated tumor targeting based on peptide hormones. *Expert Opin. Drug Delivery 7*, 79−96.
(48) Ruan, H., Hao, S., Young, P., and Zhang, H. (2015) Targeting Cathepsin B for Cancer Therapies. *Horiz. Cancer Res. 56*, 23−40.
(49) Zanella, S., Mingozzi, M., Dal Corso, A., Fanelli, R., Arosio, D., Cosentino, M., Schembri, L., Marino, F., De Zotti, M., Formaggio, F., et al. (2015) Synthesis, Characterization, and Biological Evaluation of a Dual-Action Ligand Targeting alpha(v)beta(3) Integrin and VEGF Receptors. *ChemistryOpen 4*, 633−641.
(50) Colombo, R., Mingozzi, M., Belvisi, L., Arosio, D., Piarulli, U., Carenini, N., Perego, P., Zaffaroni, N., De Cesare, M., Castiglioni, V., et al. (2012) Synthesis and biological evaluation (in vitro and in vivo) of cyclic arginine-glycine-aspartate (RGD) peptidomimetic-paclitaxel conjugates targeting integrin alphaVbeta3. *J. Med. Chem. 55*, 10460−74.
(51) Goodman, S. L., Grote, H. J., and Wilm, C. (2012) Matched rabbit monoclonal antibodies against alphav-series integrins reveal a novel alphavbeta3-LIBS epitope, and permit routine staining of archival paraffin samples of human tumors. *Biol. Open 1*, 329−40.
(52) Shi, K., Li, J., Cao, Z., Yang, P., Qiu, Y., Yang, B., Wang, Y., Long, Y., Liu, Y., Zhang, Q., et al. (2015) A pH-responsive cell-penetrating peptide-modified liposomes with active recognizing of integrin alphavbeta3 for the treatment of melanoma. *J. Controlled Release 217*, 138−50.
(53) Panzeri, S., Zanella, S., Arosio, D., Vahdati, L., Dal Corso, A., Pignataro, L., Paolillo, M., Schinelli, S., Belvisi, L., Gennari, C., et al. (2015) Cyclic isoDGR and RGD peptidomimetics containing bifunctional diketopiperazine scaffolds are integrin antagonists. *Chem. - Eur. J. 21*, 6265−71.
(54) Mezo, G., Szabo, I., Kertesz, I., Hegedus, R., Orban, E., Leurs, U., Bosze, S., Halmos, G., and Manea, M. (2011) Efficient synthesis of an (aminooxy) acetylated-somatostatin derivative using (aminooxy) acetic acid as a 'carbonyl capture' reagent. *J. Pept. Sci. 17*, 39−46.

■ NOTE ADDED AFTER ASAP PUBLICATION

Schemes 1 and 2 were inadvertantly transposed in the version published to the Web on June 19, 2019. This was corrected in the version published on July 17, 2019.

DOI: 10.1021/acs.bioconjchem.9b00292
Bioconjugate Chem. 2019, 30, 2011−2022